Renewable Energy 80 (2015) 755–769

Contents lists available at ScienceDirect

Renewable Energy

journal homepage: www.elsevier.com/locate/renene

The cumulative impact of tidal stream turbine arrays on sediment transport in the Pentland Firth

I. Fairley*, I. Masters, H. Karunarathna

College of Engineering, Swansea University, Singleton Park, Swansea SA2 8PP, UK

ARTICLE INFO

Article history:
Received 27 March 2014
Accepted 2 March 2015
Available online 23 March 2015

Keywords:
Tidal stream energy
Morphodynamics
Hydrodynamics
Numerical modelling
MIKE3
Pentland Firth

ABSTRACT

This contribution investigates the impact of the deployment of tidal stream turbine arrays on sediment dynamics and seabed morphology in the Pentland Firth, Scotland. The Pentland Firth is arguably the premier tidal stream site in the world and engineering developments are progressing rapidly. Therefore understanding and minimising impacts is vital to ensure the successful development of this nascent industry. Here a 3 dimensional coupled hydrodynamic and sediment transport numerical model is used to investigate the impact on sediment transport and morphodynamics of tidal stream arrays. The aim of the work presented here is twofold: firstly to provide prediction of the changes caused by multiple tidal stream turbine array developments to some of the unique sandy seabed environments in the Pentland Firth and secondly as a case study to determine the relationship between impacts of individual tidal stream farms and cumulative impacts of multiple farms. Due to connectivity in tidal flow it has been hypothesized that the cumulative impact of multiple arrays on sediment dynamics might be non-linear. This work suggests that, for the Pentland Firth, this is not the case: the cumulative impact of the 4 currently proposed arrays in the area is equal to the sum of the impacts of the individual arrays. Additionally, array implementation only has minimal effect on the baseline morphodynamics of the large sandbanks in the region, smaller more local sandbanks were not considered. These two results are extremely positive for tidal stream developers in the region since it removes the burden of assessing cumulative impact from individual developers and suggests that impacts to sub-sea morphodynamics is insignificant and hence is unlikely to be an impediment to development in the Pentland Firth with the currently proposed levels of extraction.

1. Introduction

Tidal stream turbines, have great potential to provide predictable renewable energy and much academic effort has focussed on their design, implementation and impacts [1]. Tidal stream turbines can only be deployed in specific resource areas where tidal current velocities exceed a certain device dependant level, typically these are in areas constrained by channels, islands or headlands [2–5]. Implementation of turbine arrays is likely to lead to areas of reduced tidal current due to energy extraction and also accelerated tidal flows in other areas due to blockage effects [6–8]. If mobile sediment is present, this might lead to changes in sediment transport regime and also to the morphology of sandy areas. Relatively little academic interest has focussed on the impacts to sediment transport compared to other areas such as hydrodynamics [7,9] or biological receptors [10,11]. Within the Pentland Firth, research has been conducted on sediment carrying capacity [12], but not on sediment transport and morphological change explicitly. The authors [12] state that research into sediment transport within the Pentland Firth should be a priority given the lack of current knowledge. Previously Neill et al. [13] used a 1D model to demonstrate that, for a relatively long channel with variations in tidal asymmetry, morphological impacts are increased if energy extraction occurs in regions of asymmetry. Case studies in the Channel Islands [14] and Anglesey [15] have used 2D coastal area models in investigate the impacts of array deployment on sediment transport and morphodynamics. Neill et al. [14] investigated the impact of large (300 MW) arrays on headland sandbanks for both idealised and realistic scenarios. They found that energy extraction of this magnitude could have significant impacts on the morphology of local sandbanks, but that careful siting of the array could mitigate this impact. Robins et al. [15] found that for smaller

* Corresponding author.
E-mail address: i.a.fairley@swansea.ac.uk (I. Fairley).

http://dx.doi.org/10.1016/j.renene.2015.03.004

array deployments of 10–50 MW the impact of energy extraction was less than the natural variability, but that as array sizes increased over 50 MW significant impacts on sediment transport were observable. They highlight the fact that results for the impact of tidal stream energy on sediment transport are case specific. This is due to the range of hydrodynamic and bathymetric and sedimentary properties of sites where energy extraction is being planned. In high energy environments suitable for tidal stream sites sediment is often spatially varying with regions of swept rock, sand and gravel [16]. Robins et al. [15]also note that use of 3D modelling would give more accurate results. Use of a 3D model allows for energy to be extracted at a specific level in the water column which allows for more realistic representation of the hydrodynamic impacts which will force changes to sediment transport.

The analysis presented here uses DHI's MIKE3 FM suite, a 3D coupled hydrodynamic and sediment transport model to investigate the impact of multiple tidal current turbine arrays on the sub-tidal morphodynamics of the Pentland Firth, Scotland (Figs. 1 and 2). This area has several tidal stream arrays in development (Table 1 and Fig. 2) and is considered to be one of the best resource areas in the world. It is described in more detail in section 2. Previously, both academic research [13,14]and commercial studies [16] into sedimentary impacts have focussed on the impact of one array, however in prime resource areas it is vital to understand the cumulative impact of multiple arrays. Clearly, such work will not be conducted by developers who only have proprietary interest in specific sites and therefore such work must be conducted by academia. In this contribution, baseline sediment transport and morphological changes over one lunar month are analysed and sub-sequentially model tests with different combinations of tidal stream arrays also tested. One aim of this contribution is to understand whether sandbanks in the Pentland Firth are likely to be affected by turbine deployment and the other aim is to test the null hypothesis:

$$I_{abcd} = I_a + I_b + I_c + I_d \quad (1)$$

where I_{abcd} is the cumulative impact of arrays a–d and I_a, I_b, I_c, I_d, the impacts of the individual arrays.

The work is presented as follows: the study area is described (section 2); the approaches taken to define sediment distribution explained (section 3); the modelling methodology is detailed (section 4); results considering baseline sediment transport are then presented before the impacts of tidal stream arrays are considered and the question of cumulative impact answered (section 5). Finally the case study is put into a global context.

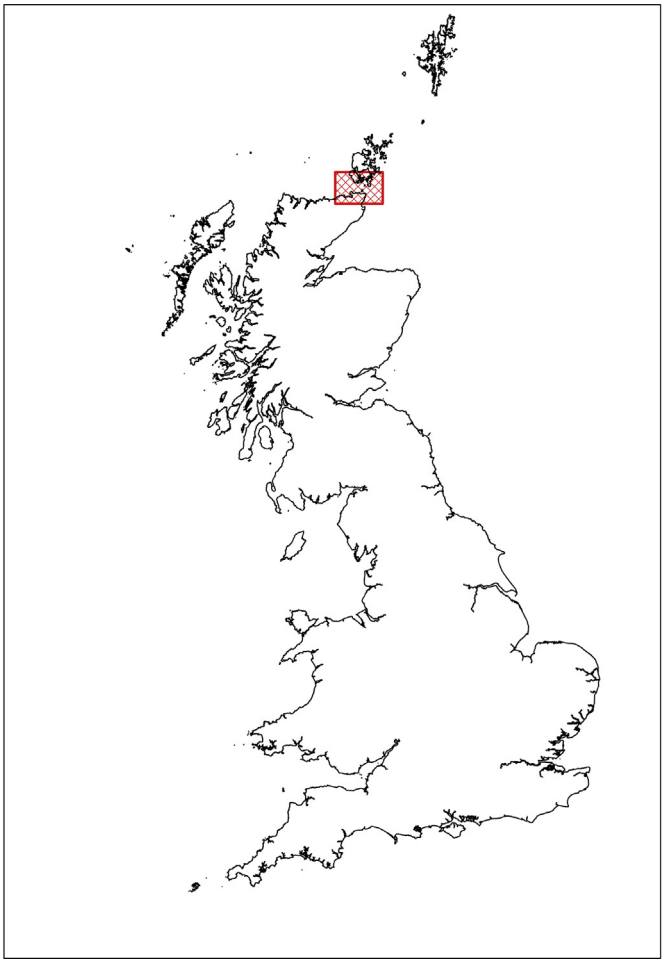

Fig. 1. The location of the Pentland Firth (red box). A more detailed map of the area is shown in Fig. 2. (For interpretation of the references to colour in this figure legend, the reader is referred to the web version of this article.)

2. Study area: the Pentland Firth

The Pentland Firth (PF) is the narrow channel formed between the Scottish mainland and the Orkney Islands that links the North Atlantic and North Sea (Fig. 1). Water depths reach −100 m from mean sea level in the centre of the channel. Mean spring tidal range at Wick, the nearest maintained tide gauge is 2.88 m. Tidal phase differences of 2 h [17] force a hydraulic gradient across the channel which drive peak spring currents which exceed 5 ms^{-1}. Flood currents are directed eastward through the PF into the North Sea and ebb currents westward from the North Sea to the Atlantic. The wave climate to the west of the region is one of the most energetic in Europe and mean significant wave heights in the Pentland Firth are 2 m [18]. Sheltering via the islands and wave blocking by the strong currents mean that wave heights in the east are lower [19]. The PF is arguably the most promising area for tidal stream development in the world: resource assessments have predicted power potential between 1 and 18 GW [20]. The methodology behind some higher estimates have been criticised [21]and Adcock et al. [22] have suggested, based on numerical modelling of rows of turbines spanning the width of Pentland Firth and utilising the metric that the time averaged power per unit swept area should be greater than an offshore wind turbine, that the maximum available power is 1.9 GW. Four tidal array projects are currently being developed in the PF and these are summarised in Table 1 and shown in Fig. 2.

Much of the PF is swept rock, and the PF has been identified as a bedload parting zone with transport directed into the North Sea in the eastern section and into the north Atlantic in the western section [23]. Nonetheless, despite the strong currents, above the threshold of motion for the observed particle sizes, there are areas of mobile sediment associated with headlands, islands or areas of weaker current. It has been recognised that elsewhere in the Orkney Islands sub-tidal sand areas are highly mobile: Farrow et al. [24] considered two surveys from the spring of 1974 and June 1977 and identified areas of bedrock in the first survey that were covered in large areas of mega-rippled sand in the second and vice versa. There are two primary areas of sediment in the PF that are the focus of this study: the Sandy Riddle to the east and an area of sandwaves to the west of the island of Stroma (Fig. 3).

The Sandy Riddle can be classed as a banner bank associated with four rocky islets named the Pentland Skerries. It is around 12 km in length and crest depths range from −16 to −60 below

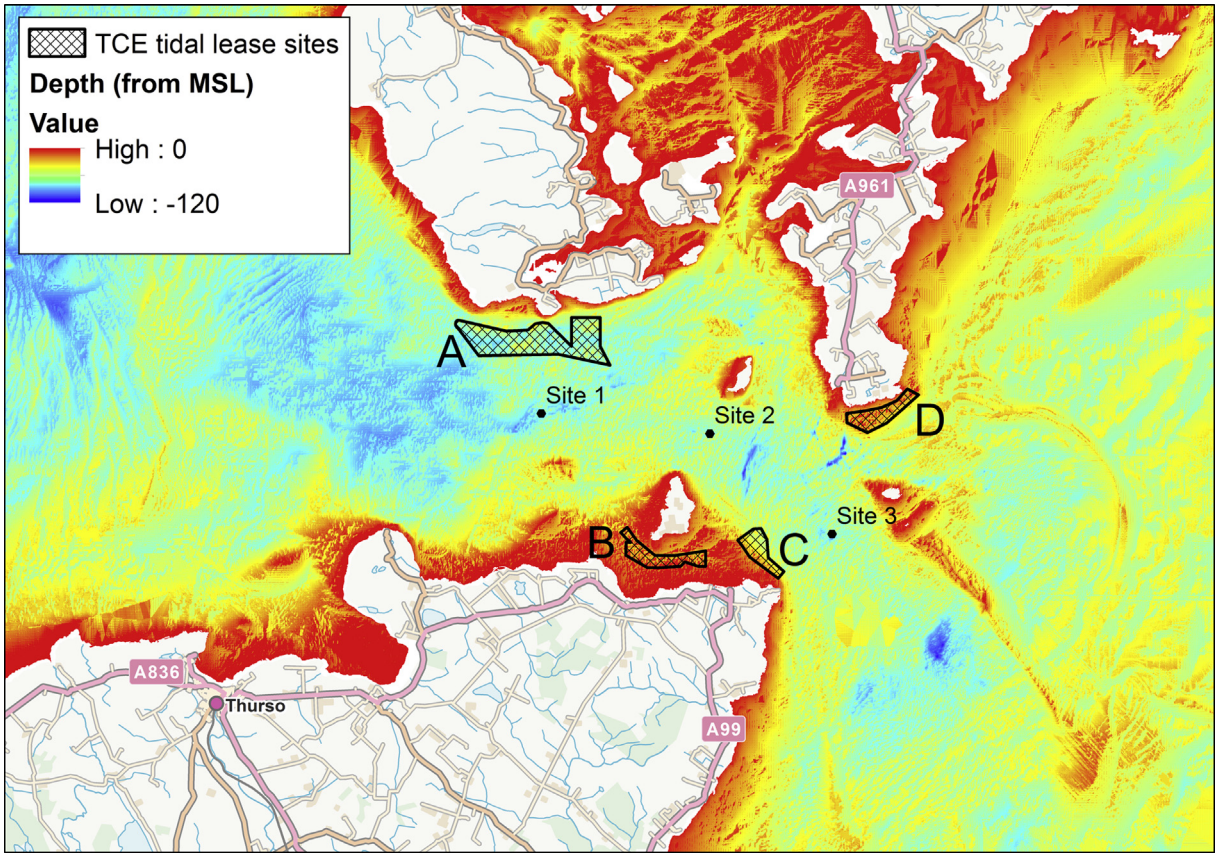

Fig. 2. Figure 2 shows the bathymetry of the Pentland Firth, the turbine deployment sites (hatched areas) and the location of the moored ADCPs used for validation (black dots). Lettering refers to the different sites which are described in Table 1. Ordnance Survey map data © Crown Copyright and Database Right 2014. Ordnance Survey (Digimap Licence).

mean sea level. The bank is covered in sandwaves and mega ripples. Much of the mobile sediment in the region is composed of coarse sand to gravel sized shell fragments and highly calcareous sand [25]. Flather [26] suggests that under storm surge conditions strong easterly driven flows will be superimposed on the strong tidal currents. Additionally, Light and Wilson [25] report that linear wave theory suggest sediments would be mobilised up to a depth of 200 m by the 50 year return period wave conditions and therefore larger wave events could also impact on sediment transport over the shallower Sandy Riddle. Therefore it has been surmised [27] that the crest of the Sandy Riddle would be the most active region for bedload transport in the area.

As far as the authors are aware, no attention has been given to the area of sandwaves west of Stroma. They cover an oval shaped area 4 km long by 2 km wide and consist of medium to coarse sand. The crest of the sandbank containing the sandwaves is −25 m MSL with deeper areas around 70 m based on multibeam data collected by Marine Scotland Science in 2009. The area is unsheltered from swell and wind waves coming from the North Atlantic. The most defined sandwaves are present on the northern flank, with wavelengths ranging from 150 m in the west to 400 m in the east. The sandwaves are saw-toothed in shape with the steeper slope to the east, indicating a residual eastward transport along that flank. The sandwaves on this flank arise from bifurcations of less regular sandwaves over the crest and southern flank.

Table 1
A summary of the four tidal stream turbine arrays currently proposed in the Pentland Firth. Where data is unavailable, fields have been left blank.

	Brims tidal array	Meygen inner sound	Ness of Duncansby	Brough Ness tidal array
Map reference	A	B	C	D
No. turbines	200 (60)	86	95	66
Total capacity (MW)	200 (60)		95	99
Device	Open hydro	Unnamed	Hammerfest Strom	MCT
Device rating (MW)	1	1–2.4	1	1.5
Diameter (m)	20	16–20	21	2 × 16
Hub height (m)	17	13.5–16	22	
Lateral spacing			2.5D	
Longitudinal spacing			10D	

3. Definition of sediment size and spatial coverage

A significant problem for modelling studies involving sediment transport in areas such as the Pentland Firth is the highly spatially variable nature of the natural sediment in terms of both abundance and grain size. Within the model domain are a wide range of seabed types including but not limited to: swept bedrock areas, sand veneers on bedrock, large cobbles with interstitial sand and gravel, large sandbanks and sandwave fields. Unfortunately data availability in the area is poor, with sparse point data of varying quality. Two aspects need to be considered for application into the model: maps of erodible sediment areas and maps of the spatial variation in grain size. These are considered separately below.

3.1. Spatial variation in mobile sediment

In areas such as the Pentland Firth, it is insufficient to interpolate between sparse sediment samples and assume uniform

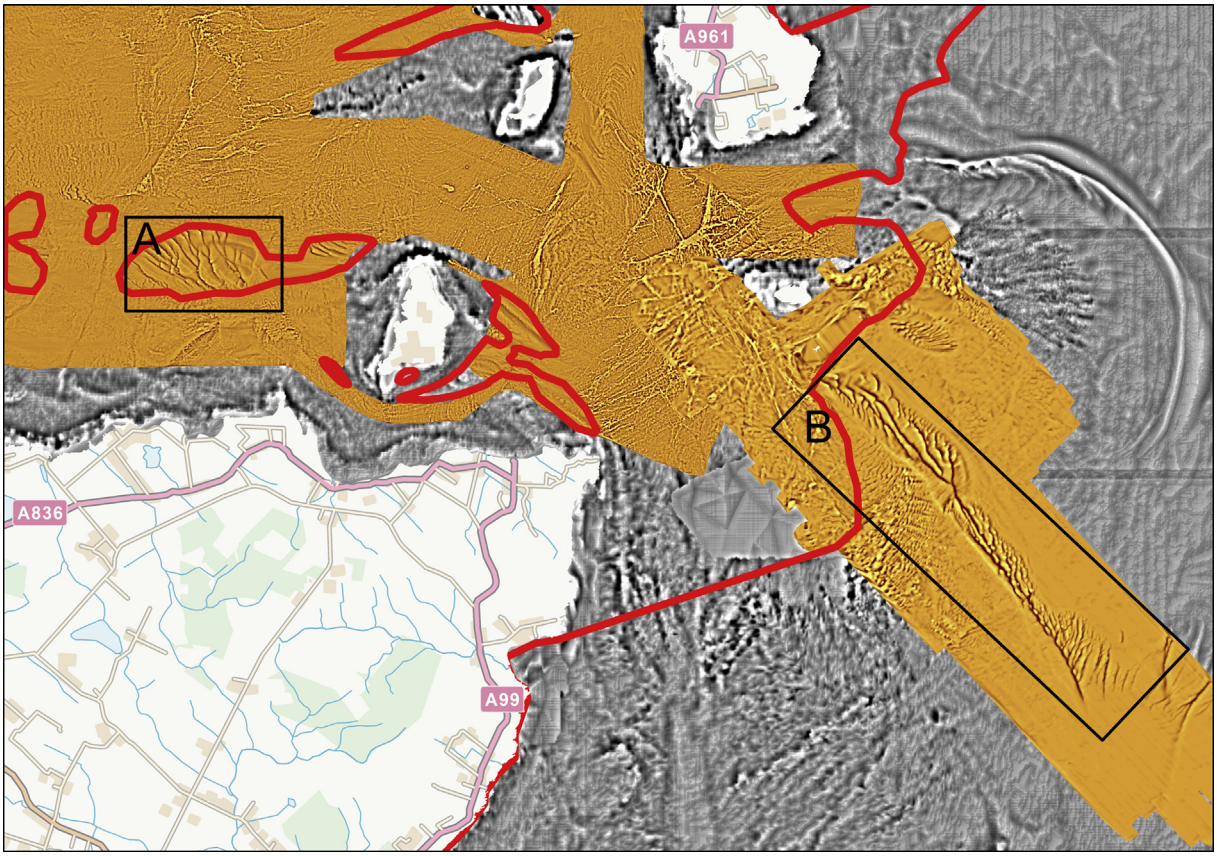

Fig. 3. A plot of the model area showing the textural surface used to identify mobile sediment areas based on the presence of sand waves/ripples. The sand coloured area is the area covered by multibeam data and the grey area the area where a 20 m grid was used. The area marked A is the sand wave area and the area marked B is the Sandy Riddle. The red line indicates the edge of areas defined as sand in the textural classification. (For interpretation of the references to colour in this figure legend, the reader is referred to the web version of this article.) Ordnance Survey map data © Crown Copyright and Database Right 2014. Ordnance Survey (Digimap Licence).

sediment coverage: there are substantial areas of swept bedrock, with deeper sediment deposits in the lower flow areas. For a complete description of the sedimentary regime, sub-bottom profiling to determine mobile sediment layer thickness would be required. This is unavailable in the model domain and hence inference from other data was required. De-trended high resolution bathymetry was used to provide a textural surface which can be used to infer seabed type given that point sampling was too spatially sparse. Where multibeam echosounder data was available, it was interpolated onto a regular grid with 3 m spacing, otherwise a 20 m gridded bathymetry supplied by the crown estate was used [28]. The multibeam datasets used were the Pentland Firth coverage collected by Marine Scotland Science, coverage of the Sandy Riddle collected by the British Geological Survey and data collected by UKHO. A smoothed bathymetry surface was produced by applying a moving window average to the gridded data and this surface used to de-trend the gridded bathymetry and produce a textural surface (Fig. 3). Different sediment types are clearly observable in this surface, with sand areas indicated by very smooth surfaces or rippled surfaces whereas bedrock areas are indicated by an irregular, creviced surface. This methodology was ground-truthed using available data from Marine Scotland Science video trawls in the region (Fig. 4). Therefore the spatial extent and distribution of sand patches could be manually defined in a GIS package (Fig. 3). More sophisticated automatic classification techniques have been suggested [29,30], however these require access to backscatter data as well as bathymetry which was not available in this instance.

3.2. Sediment size distribution

Two data sources were available for sediment size, the British Geological Survey's seabed samples and the Marine Scotland (MS) database of benthic video trawls which included a seabed descriptor. The BGS data had two levels of accuracy: some had a phi class-weight table from which median grain size d_{50} could be estimated, others only had a Folk classification [31]. For those with a Folk classification and no weights, $d50$ was ascribed based on median values for sand, gravel and mud within the Folk classification. Similarly, for the MS bethic surveys, a d_{50} was assigned based on the median value of the seabed descriptor on the ISO sediment scale, e.g. if the seabed descriptor was 'medium sand' a grain size of 0.415 mm was assigned to that location. While clearly these two latter methods are less accurate than measured grain size, it is believed that having a better spatial coverage far outweighed this lack of accuracy. Sediment size was then interpolated between these points before the previously established sand areas were used as a mask to remove bedrock areas. Fig. 5 shows a map of the study area with interpolated grain size and the location of the MS video trawls and BGS point samples.

4. Modelling methodology

4.1. Model description

DHI's MIKE series of models are a set of industry standard 'black box' numerical models that include various modules for

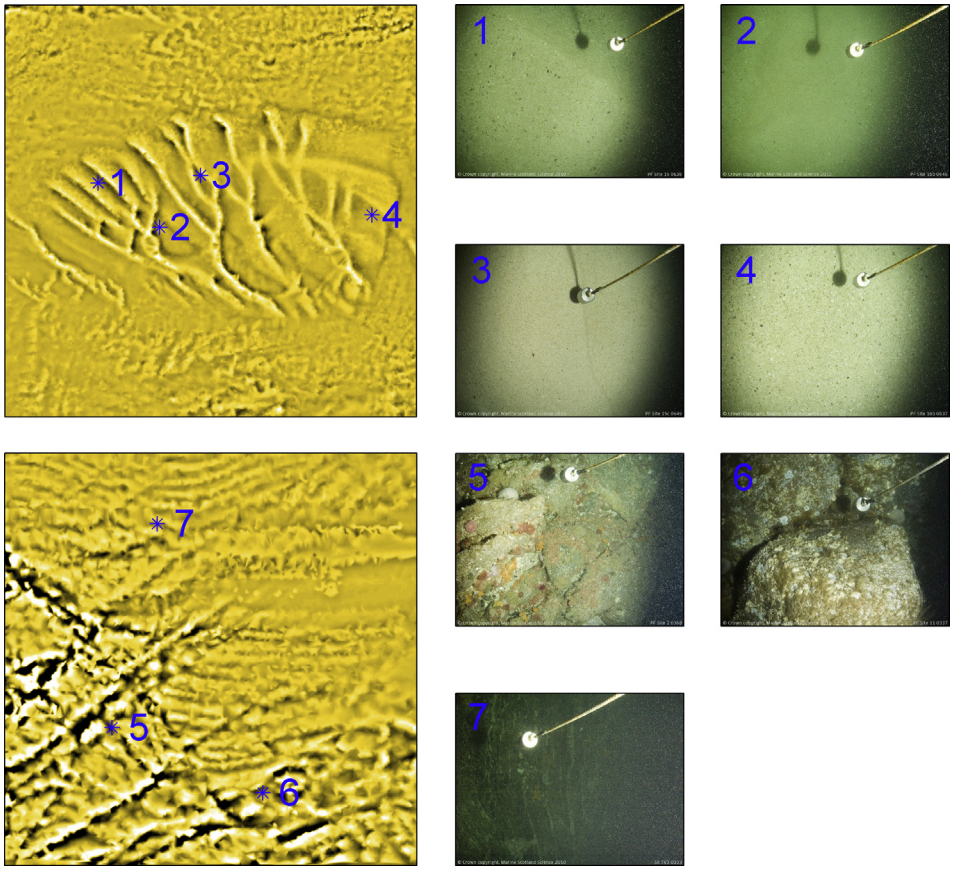

Fig. 4. Ground-truthing of the textural classification, with the textural surface for a sand area in the top left, a textural surface for a rock area on the bottom left and images from Marine Scotland video trawls showing the bottom type.

hydrodynamics, sand and mud transport and various wave models [32]. This suite of models has been actively used in the marine renewable energy field [33–36] as well as in coastal engineering [37], flood management [38]and coastal processes [39]. In this study, the three dimensional flexible mesh (FM) hydrodynamic (HD)and sand transport (ST) modules are used. The MIKE3 FM suite uses a cell centred finite volume unstructured triangular mesh. In this study, vertical resolution is provided via a sigma level co-ordinate system to allow for a free surface. The model also caters for a z-level or mixed z and sigma level vertical co-ordinate system.

The HD module solves the three dimensional incompressible Reynolds averaged Navier Stokes equations, following the assumptions of Bousinesq and hydrostatic pressure. Full details of the model equations and numerical scheme can be found in Ref. [40]. The higher order solution technique was used following DHI's recommendations that such a scheme should be used when convection is important [41]. Flooding and drying was incorporated using the default values of 0.005 m drying depth, 0.05 m flooding depth and 0.1 m wetting depth. Horizontal eddy viscosity was handled using the Smagorinksy formulation [42] with a constant of 0.8 and vertical eddy viscosity utilised a log-law formulation [40]. A roughness height formulation was used for the bed resistance with values varying over the domain, around the coastline a roughness of 4 m was used and elsewhere the roughness was set to 2 m. While this value is large, it is appropriate in this region given the prevalence of irregular bedrock. Water levels were used as boundary conditions (section 4.3) due to the currents in the PF being forced by the hydraulic gradient between North Atlantic and North Sea [17].

The sand transport model takes current forcing and bed resistance from the hydrodynamic model [43]. Maps of sediment size and distribution were created based on the analysis presented in section 3. Sediment transport is calculated using the van Rijn equations for suspended and bedload transport [44,45] and the depth averaged current velocity from the hydrodynamic model. Again a higher order solution technique was used due to the importance of convective flow [43] A more conventional value of bed resistance is used for the sediment transport calculations compared to the hydrodynamic simulations: the default MIKE setting of a Manning number of 32 $m^{1/3}/s$ was used. This difference is because the majority of the hydrodynamic simulation is impacted upon by the large roughness of the bedrock areas, where the sediment transport occurs in areas where conventional bed roughness associated with sandy areas are applicable.

The two models are fully coupled at each time-step such that computed changes to bed level are fed to the hydrodynamic module to allow for accurate prediction of currents.

For all model tests the model was run from 11/09/2001 00:00:00 until 15/10/2001 17:20 using a time step of 60 s. This time period was used due to the availability of ADCP data for validation. A model spin-up of 48 h was used before the sediment transport and morphological updating was activated.

4.2. Model domain and mesh

A triangular mesh was developed using DHI's MIKE mesh generator and optimised using a MATLAB toolbox provided by DHI. Areas where turbines would be deployed or areas with mobile

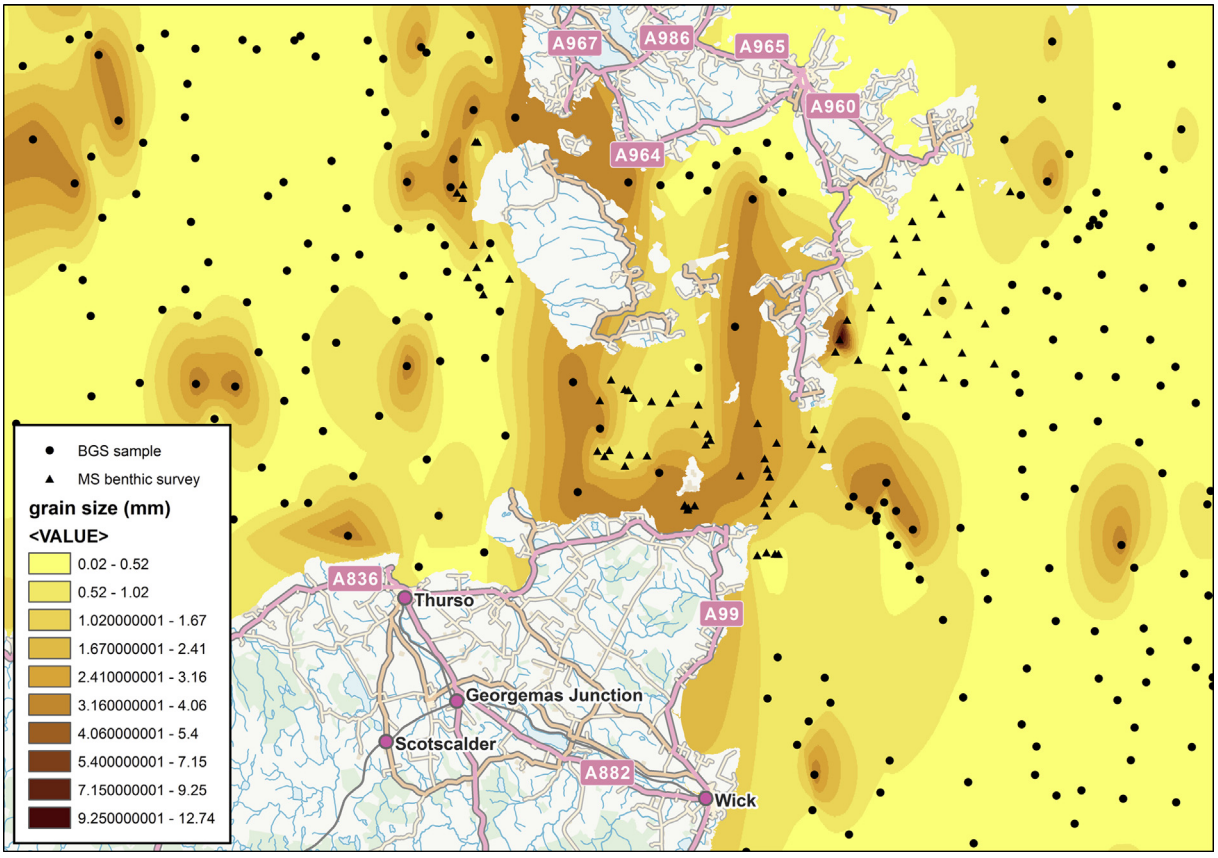

Fig. 5. Sediment size distribution based on BGS sediment samples and Marine Scotland seabed classifications. Ordnance Survey map data © Crown Copyright and Database Right 2014. Ordnance Survey (Digimap Licence).

sediment were prescribed higher grid resolution (Fig. 6). The computational expense of running coupled hydrodynamic-sediment transport models in three dimensions meant practical concerns restricted the size of the model domain. Therefore, the model domain was sized such that the current jet of the Pentland Firth was enclosed within the domain and Scapa Flow was excluded from the analysis. Verification against ADCP data provided confidence in the baseline case with no turbines in place (section 4.4) despite the size of the domain. Arguments have been made that model domains should be made as large as possible to reduce the influence of boundary effects on marine energy installation modelling [46], however the time constraints of running the model on a desktop PC mean this was unachievable. In order to verify the applicability of the domain selected, a 3D version of the TCE model (section 4.3) was run with and without turbines in place to examine differences caused by the smaller domain. A comparison is made in

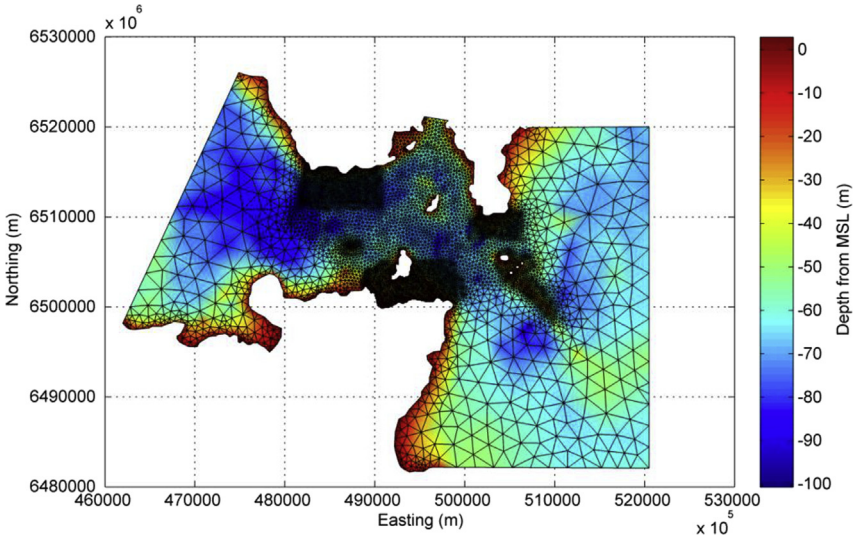

Fig. 6. The model mesh and bathymetry used in this study.

the difference between the baseline (no turbine case) and the model run with all four arrays at peak flood and ebb currents (Fig. 7). It should be noted that in this paper the nautical nomenclature will be used such that flood denotes the portion of the tidal cycle progressing from low tide to high tide and ebb denotes the portion of the tidal cycle progressing from high tide to low. While there are some differences noticeable in the array near field, there are minimal changes in mean current speed difference over the mobile sediment areas considered in this work: for the sandwave area the difference in change between the two domains is 0.0007 ms^{-1} on the flood and 0.018 ms^{-1} on the ebb; for Sandy Riddle the difference is 0.01 ms^{-1} on both the flood and ebb. This is less than 0.5% difference in all cases.

4.3. Boundary conditions

Hydrodynamic boundary conditions were generated from a 3-dimensional version of the PFOW tidal model that was built by ABPMer for The Crown Estate [18,28,36]. The 2D version has been extensively validated and reported upon [36]. The same model set up, boundary conditions and mesh was used (Fig. 8), but the model was run in 3D mode with 10 sigma levels in order to get boundary conditions for the local mesh. The only alteration to the set up was the use of roughness length instead of Mannings number (M) for the bed resistance. The difference was due to differences in model options for 2 and 3 dimensional set-ups. The roughness length (k_s) was calculated from the Manning's numbers in the original set-up using:

$$M = \frac{25.4}{k_s^{1/6}} \tag{2}$$

Boundary conditions were taken from DHI's global tide model and water levels to be used as boundary conditions for the PF model extracted from the larger TCE/ABPmer model (shown as black lines in Fig. 9).

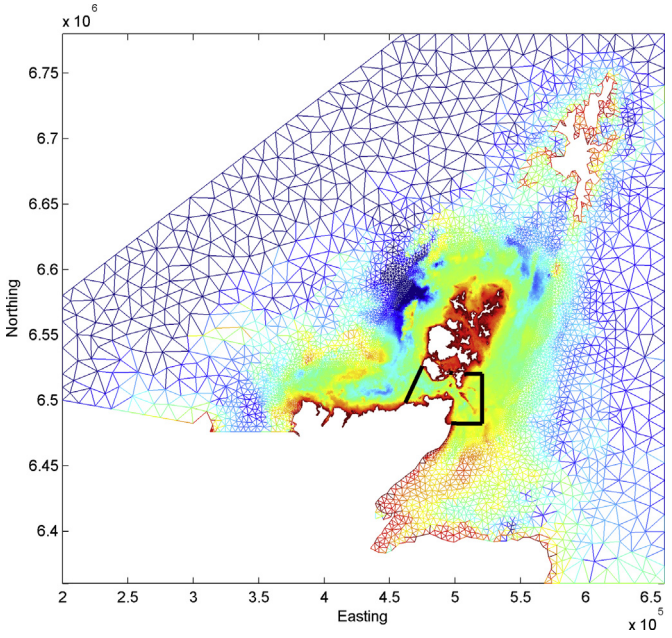

Fig. 8. A map showing the mesh used in the ABPmer/TCE study which was used to provide boundary conditions for our local model. The black lines indicate model boundaries for the local mesh.

For the sand transport model the morphological boundary conditions were set to zero sediment flux gradient and the sediment transport to equilibrium conditions.

4.4. Model validation

Only the hydrodynamic model could be validated due to the scarcity of sediment data or repeated morphology surveys in the Pentland Firth. The hydrodynamic model was validated against

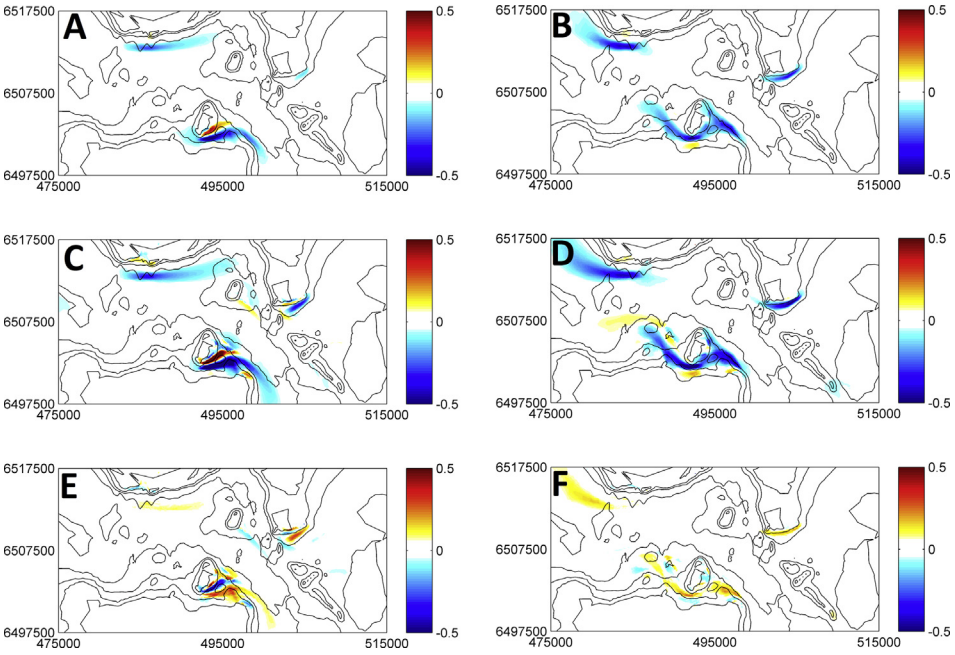

Fig. 7. A plot showing the difference in depth averaged current speed (ms^{-1})between the case with turbines and with no turbines for A) the mesh used in this study on a peak spring flood current, B) the mesh used in this study for a peak spring ebb current, C) the TCE mesh on a peak spring flood current, D) the TCE mesh for a peak spring ebb current, E) the difference between the two meshes for the flood case, F) the difference between the two cases for the ebb case.

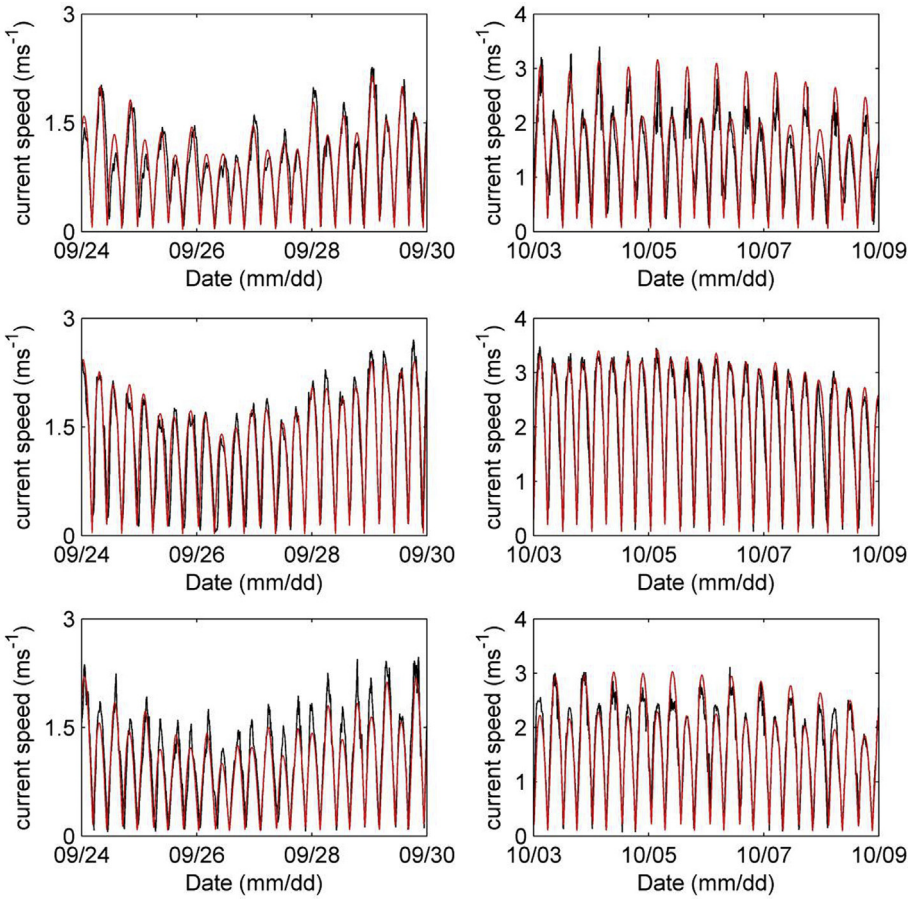

Fig. 9. Plots of depth averaged current speeds (ms^{-1}) for spring (right hand side) and neaps (left hand side) for site 1 (top), site two (middle) and site 3 (bottom). Model results are drawn as red lines and measured results as black lines. (For interpretation of the references to colour in this figure legend, the reader is referred to the web version of this article.)

three moored ADCPs deployments in the centre of the Pentland Firth (Fig. 1) from September–October 2001. RDI Workhorse Sentinal 300 kHz ADCPs were used, suspended above the seabed with 100 kg lift low drag sub surface buoys. It has been reported by the data providers that the ADCPs suffered from 'knock-down' at times of peak current speed and while this was corrected for there might be some errors at these times. Fig. 9 shows a comparison between measured and modelled depth averaged current speeds for all three sites over temporal subsets covering spring and neap periods. It can be seen that in general the agreement between measurement and model is good. Site 2 matches most closely ($r^2 = 0.96$, root mean square error (RMSE) = 0.26 ms^{-1}) whilst site 1 ($r^2 = 0.92$, RMSE = 0.33 ms^{-1}) and site 3 ($r^2 = 0.95$, RMSE = 0.27 ms^{-1}) perform slightly less well due to a slight under-prediction of peak currents on neap tides and a slight over-prediction of peak currents on spring tides. This over prediction occurs on opposite halves of the tidal cycle and could either be due to the measurement knock-down error or difficulties of modelling the current jet caused by the Stroma constriction. Other modelling studies have reported similar errors [47] There is a phase difference between modelled and measured data of approximately 7 min.

4.5. Turbine implementation

Arrays are represented as groups of individually specified turbines (location, hub height, turbine diameter and drag co-efficient). The in-built tool for the specification of tidal turbines in MIKE3 is used in this study to implement the turbines as sub-grid structures – grid spacing was such that each turbine occupied a single horizontal cell with only one turbine per cell. The turbines are implemented as a momentum sink based on actuator disk theory [48]. Actuator disk approaches have been applied to aviation and nautical propellers [49,50], wind farms [51,52] and more recently tidal stream turbines. Actuator disk theory gives a simple 1 dimensional approach to rotor modelling by considering the rotor as a discontinuity in the fluid [53]. The main assumptions of the technique are: the rotor can be considered as an infinitesimally thin disk of a prescribed area; frictional forces can be considered negligible compared to changes in pressure and momentum; thrust loading and velocity are uniform over the disk; flow is incompressible, irrotational, inviscid and isotropic; and in the far field the fluid is at free-stream pressure [54]. Readers further interested in actuator disk theory are directed to [55–61]. Importantly to this study, several studies have demonstrated the value of RANS – actuator disk models for environmental impact assessment [53]. While the assumptions needed for actuator disk theory can lead to inaccuracies in the near-field wake [53], close similarities between far-field actuator disk wakes and far-field wakes from rotating horizontal axis turbines has been reported [55], this means the approach is suitable for examination of far-field impacts on sediment dynamics.

There are options within MIKE3 to either include the turbines as a constant drag co-efficient or with a variable lift and drag co-efficient. In this study the simpler approach of specifying a constant drag co-efficient was used. The drag force (F_D), from actuator disk theory, is calculated by:

$$F_D = \frac{1}{2}\rho_w \alpha C_D A_e V^2 \quad (3)$$

where ρ_w is the density of water, α is a correction factor that is equal to 1 in this study, C_D is the drag co-efficient, A_e is the effective area of the turbine and V is the velocity. This drag force can then be used to implement a sink in the momentum equations via an additional source term to approximate the energy extraction by a tidal turbine. MIKE3 is a 'black box' commercial code and therefore the exact specifics of the implementation of the additional source term is not obtainable.

The sink is evenly distributed between the vertical layers covered by the turbine swept area [48]. The velocity V is taken as the average of the velocity over the portion of the water column occupied by the turbine. In this study turbine diameter was taken as 20 m and the hub height as 17 m. A constant drag co-efficient of 0.6 was used. Sensitivity tests were conducted for C_D between 0.3 and 0.9 but differences to depth averaged current speeds were less than 0.03 ms^{-1} in the two areas of mobile sediment considered.

Array spacing between turbines for three of the sites were taken to be 2.5D laterally and 10D longitudinally based on information about the Ness of Duncansby site [62], where D is the turbine diameter. Layout for the Meyen site was based on an indicative layout provided in their environmental statement [16] and hence an approximation of this layout was used in the study. The four array layouts used in this study are shown in Fig. 10.

5. Results

In this section, results of the modelling exercise will be presented. Firstly results showing the sediment transport over the PF area with and without farms will be presented and secondly results considering cumulative impacts will be presented. Hydrodynamic results are not considered in detail, apart from for the section on cumulative impacts, given the body of work dealing explicitly with hydrodynamics of the Pentland Firth, which is being extended within another work package of the Terawatt project. For descriptive purposes Fig. 11 shows peak flood and ebb current speeds and directions for a spring tide. The primary current feature is the current jet between the island of Stroma and the Orkney mainland. This jet is directed South East on the flood and West on the ebb.

Attention will largely be focused on the two large areas of mobile sediment in the Pentland Firth: Sandy Riddle and the sandwave field to the west of Stroma. Fig. 12 shows the bed level change over the entire model run time for the region without turbine installations. It can be seen that the largest and most defined changes are observed in these two areas, with little change elsewhere due to the presence of large amount of bedrock. This plot shows the validity of focussing the analysis on these two locations for the remainder of the results.

Fig. 10. Tidal energy turbine array layouts for (A) the Brims tidal array, (B) the Brough Ness tidal array, (C) the Meygen array and (D) the Ness of Duncansby array. Turbines are marked as black dots and the licensed areas as black lines.

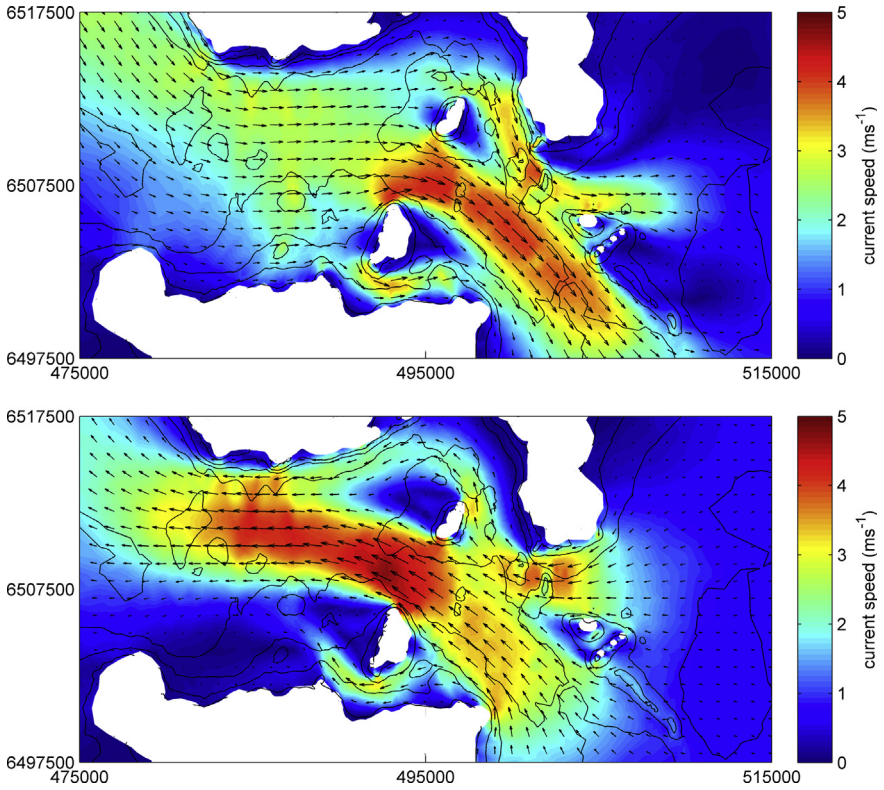

Fig. 11. Current speeds (ms^{-1}) and directions for flood (upper) and ebb (lower) peak spring conditions. Colour shading indicates current speed and vectors direction. (For interpretation of the references to colour in this figure legend, the reader is referred to the web version of this article.)

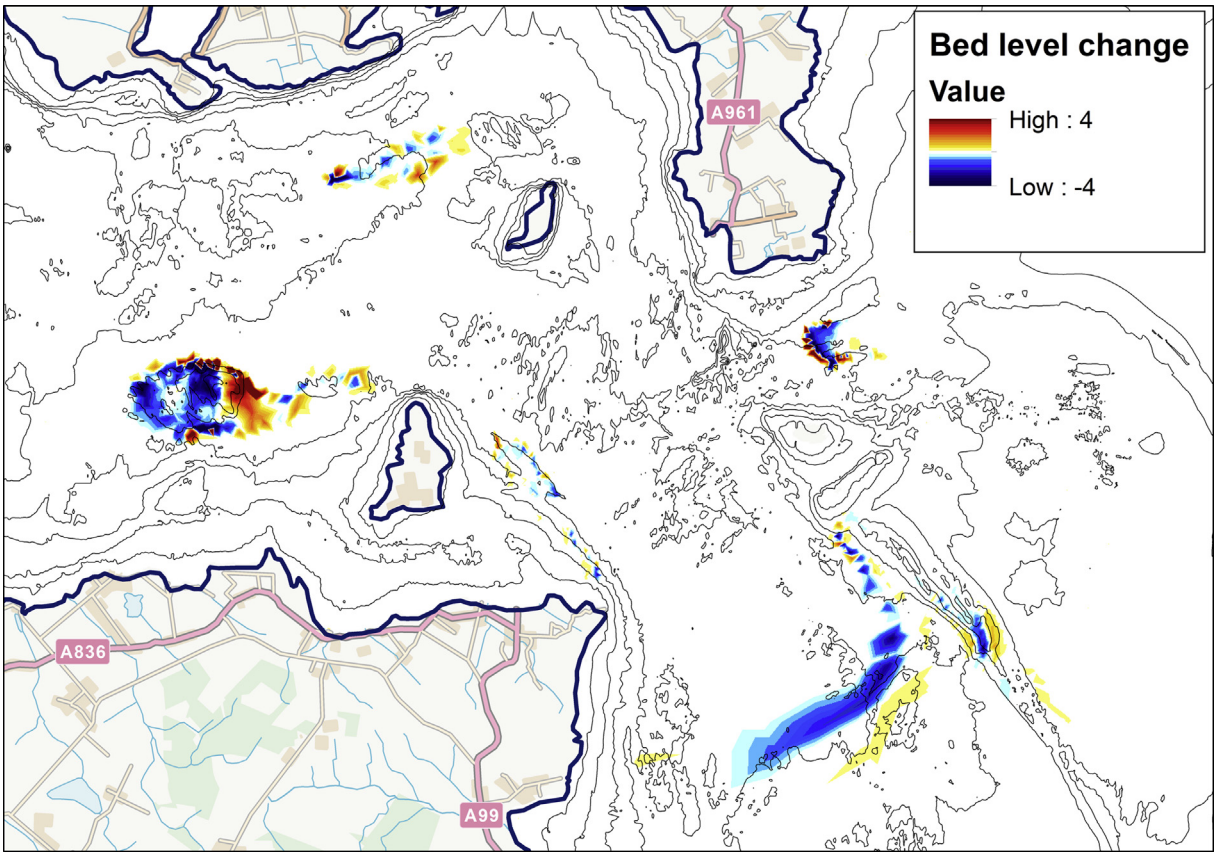

Fig. 12. A plot of bed level change (m) over the entire model run between 13/09/2001 and 15/10/2001. Ordnance Survey map data © Crown Copyright and Database Right 2014. Ordnance Survey (Digimap Licence).

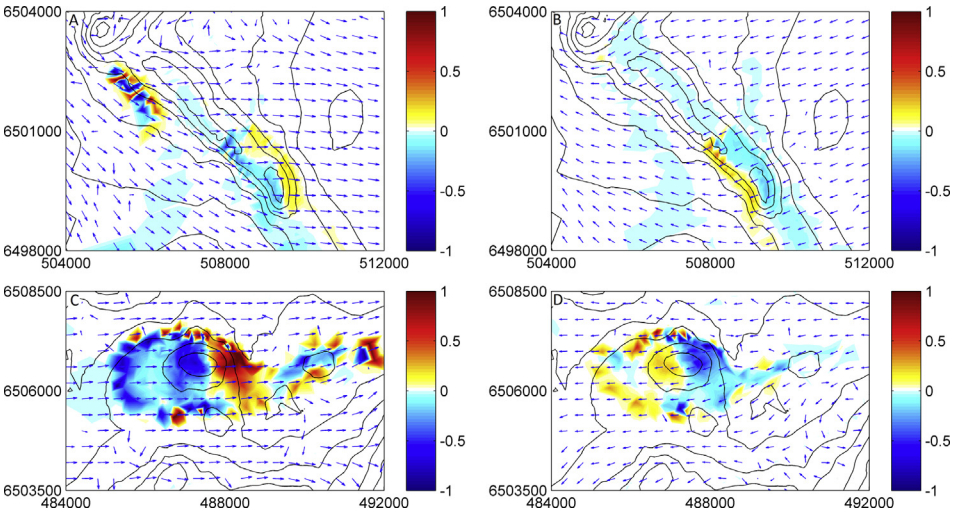

Fig. 13. Rate of bed level change in m/day and direction of total load transport for peak spring flood currents (a&c) and peak spring ebb currents (b&d) for Sandy Riddle (a&b) and the sand waves west of Stroma (c&d). The two areas are marked in Fig. 3.

5.1. Sediment transport under natural conditions

Fig. 13 shows the rate of bed level change (m/day) for peak flood and ebb currents on a spring tide. Vectors show the corresponding direction of total load transport. Fig. 14 shows the same plot for neap tides. It can be seen that the majority of change occurs over spring tides. On neap tides rate of bed level change is largely under 0.1 m/day compared with changes approaching 1 m/day on spring tides. On neap tides it is only over the sandwave area on a flood tide where larger rates of change (0.3 m/day) occur.

On spring tides, during flood tide there is erosion on the western flank of the tip of Sandy Riddle and accretion on the eastern flank. On the ebb tide the reverse occurs. At both stages of tide there is some erosion of the crest. Magnitude of rate of change is similar for both flood and ebb which suggests that the bank is remains in the same position. On neap tides there is slight erosion along the crest of the bank for both the flood and ebb tide but this change is small.

Over the sandwave region, erosion occurs on the western half and accretion on the eastern half for flood tides and the reverse on ebb tides. Magnitude of change is greater on the flood tide for both spring and neap tides. This means that there is a net transport from west to east over the tested lunar month.

The resulting changes to seabed level over the lunar month between 13/09/2001 and 11/10/2001 (two spring-neap cycles) is shown in Fig. 15. Changes are greater in magnitude over the sandwave region compared to the Sandy Riddle: maximum change in the sandwave area is 3.8 m compared to a maximum change of 2.9 m on the Sandy Riddle. On the Sandy Riddle there is erosion of the crest on the tip and accretion on the flanks. For the sandwave area there is accretion to the east and erosion to the west.

5.2. The impact of installing tidal stream arrays on sediment transport

Installation of the four arrays of turbines impacts the sediment transport and morphological changes at both the Sandy Riddle and sand wave areas.

Fig. 16 shows the bed level change over the tested lunar month with all four farms activated for the two areas of interest and the difference between the cases with and without turbine arrays given

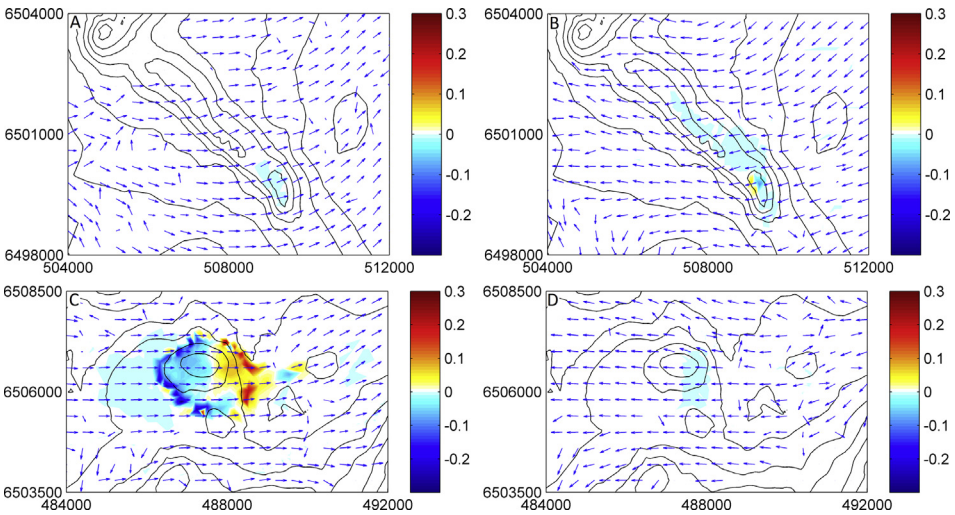

Fig. 14. Rate of bed level change in m/day and direction of total load transport for peak neap flood currents (a&c) and peak neap ebb currents (b&d) for Sandy Riddle (a&b) and the sand waves west of Stroma (c&d).

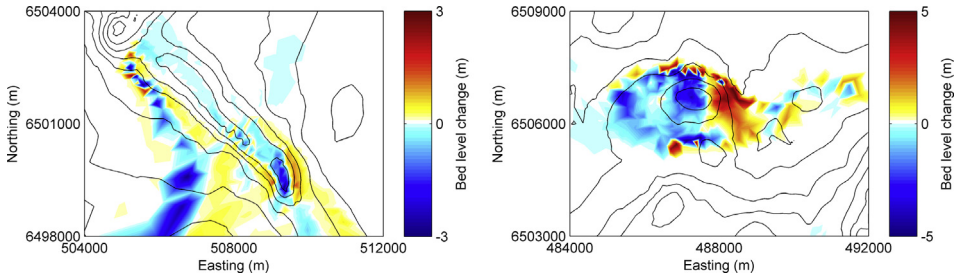

Fig. 15. Total bed level change over the tested lunar month between 13/09/2001 and 11/10/2009 for the Sandy Riddle (left) and the sand wave area (right).

in Fig. 11. Patterns of bed level change are very similar to the case with no farms present (Fig. 15), however over the Sandy Riddle the magnitude of change is slightly less whilst over the sand wave field changes are generally less apart from a small area of increased change on the northern edge. These changes are all less than 0.2 m, which is small compared to the bed level changes over the tested lunar month. Over the entire domain the root mean square difference (RMSD) is 0.0596 m, for the sand wave area the RMSD is 0.1778 m and for the Sandy Riddle the RMSD is 0.0313 m.

5.3. Consideration of cumulative impacts

One question that is of key importance in areas such as the Pentland Firth is the linearity of cumulative impacts caused by multiple farms. This is tested here by comparing the sum of impacts caused by each individual farm with the impact of all four farms together. Fig. 17 shows the difference in change to depth averaged current speed for the case when all four farms are modelled together compared to the sum of the farms modelled individually for peak flood and ebb current speeds on a spring tidal cycle. It can be seen that there is little (of order 0.01 ms^{-1}) difference in predicted impact whether the different arrays are modelled individually or all in one model. However on the ebb tide there are differences over the sand wave region and on the flood tide there is marginal differences over the crest of Sandy Riddle. Since these differences are instantaneous, it is plausible that over a long time period there might be implications for the sediment transport and sub-tidal morphology. It should also be noted that differences are concentrated around the Meygen inner sound and Ness of Duncansby arrays which are in much closer proximity than the two on the northern edge of the Pentland Firth.

In order to consider the difference between modelled cumulative impact and summed individual impacts for sediment transport, plots (Fig. 18) are presented of the difference in total bed level change over a lunar month for the two cases for both the Sandy Riddle area and the sand waves west of Stroma. It can be seen that the difference is minimal, being less than 2 cm, and that for the Sandy Riddle there is no pattern to this difference. For the sand wave case, the summation of the individual impacts gives slightly greater change over the centre of the bank and lesser change around the flanks. This difference is about 1/10th of the difference between the natural and turbine case and this it is not considered significant. The RMSD between the two cases is 0.0032 m for the sandwave area and 0.0025 m for the Sandy Riddle.

6. Discussion

This study has used a 3D numerical model of the Pentland Firth to develop understanding of the morphodynamics of the region and the potential impact of tidal stream energy extraction on subsea morphology. Accurate modelling of the hydrodynamics was achieved via calibration and validation of the model against measured data. It has been shown that the model performs well against three ADCP records (section 4.4). Some discrepancy at peak currents was noted; however it is believed that this is, at least in part, due to equipment errors caused by knock down of the floating mounting platform under peak flows and other measurement errors. It should be noted that calibration of the morphodynamic

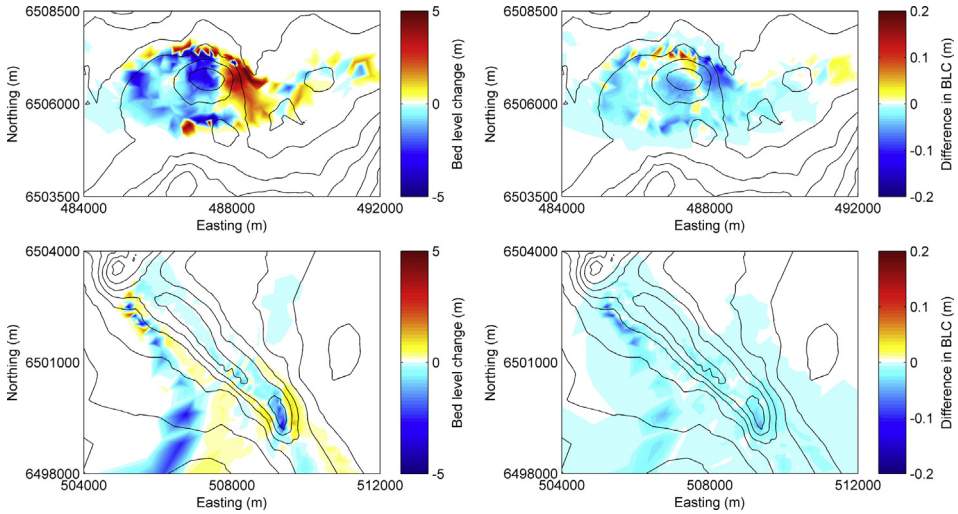

Fig. 16. Bed level change with four farms activated for the sand wave area (top left) and Sand Riddle (bottom left) and difference in bed level change between the farm and no farm case for the sand wave area (top right) and the Sandy Riddle (top left).

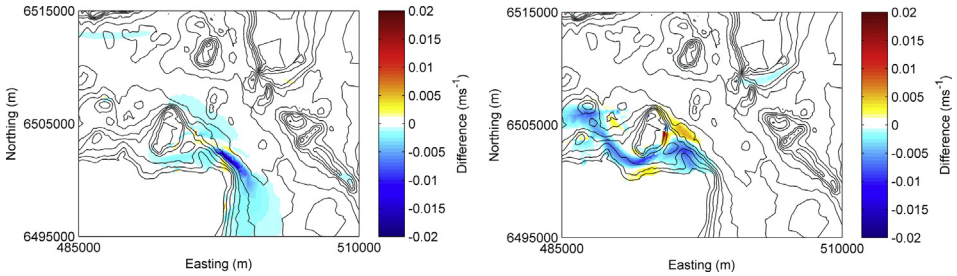

Fig. 17. A plot of difference in the difference in current speed between a model run including all four farms and the sum of the four farms modelled individually at peak spring flood current (left) and at peak spring ebb current (right).

model is not possible to due to lack of necessary data in the geographic area concerned. Calibration and verification of morphological models in scenarios such as this would rely on two possibilities: comparison with measured sediment transport rates at a certain points and comparison against observed morphological changes over a specified area or set of profiles or transects. Collection of either type of data would be expensive in environments as energetic as the Pentland Firth. Calibration against a small number of point measurements of sediment transport might be of limited value given the spatial variation is sediment size and coverage. Comparison against measured morphological change over a specified sandbank area, should such data become available, would be more appropriate. Such an approach would allow for understanding of patterns, magnitudes and directions of change. MIKE uses well calibrated and widely used sediment transport formulations, which are applicable to a wide range of seabed conditions, however, the tools are more commonly used in areas of greater sediment supply and the authors are not aware of the use of MIKE3 to predict sediment transport in areas of sparser sediment such as the Pentland Firth. Therefore, not only must results be interpreted with caution, but any future verification of results would be useful to the wider community.

Beyond accurate representation of the hydrodynamics, the validity of any renewable energy impact study rests on the description of energy extraction. Equally important in this case is the description of the sediment properties over the entire model domain. These two considerations are discussed below.

The model used, the Danish Hydraulic Institutes MIKE3 suite, is an industry standard model for coastal engineering and marine environmental impact studies. Increasingly the model is being adopted by the tidal energy industry and as such, it has in-built functionality for the implementation of turbines as sub-grid structures in the model domain. Two levels of detail are available for turbine description: in this study the simpler constant drag approach is used due to a lack of available data on lift and drag curves. Should lift and drag curves be available, a more realistic description could be used: previous work [63] has shown that a variable thrust co-efficient reduces the amount of energy dissipation by an array. However for this work sensitivity tests suggest that the difference to morphological results would be small. Also, the focus here is not on a specific device but generic tidal energy extraction as a whole. As a result, it was decided that in this case the simpler description of extraction was still relevant. The model caters for the description of individual turbines and so arrays must be specified on a turbine by turbine basis. This means that array layout will have a bearing on results. Previous work has shown that array shape also influences hydrodynamic impacts [64]. In this study, turbine layout for one site was based on an indicative layout and for the other sites spacing between turbines was prescribed as 2.5D laterally and 10D longitudinally. Not only was this spacing suggested in developers documents [62], but academic work has suggested a staggered lattice with this spacing is a good array layout [65–67]. The arrays do not fill the consented areas and hence there is the potential for changes to results caused by micro-siting and changes to both array spacing and array layout [64], for example regular grids or non-uniform layouts (e.g Ref. [68]). Until array designs and locations are finalised, exact level of impact for the current scenario cannot be predicted, however given the limited impact predicted, it is not believed that micro-siting will affect the conclusion significantly assuming that numbers of turbines do not change. The level of extraction investigated here is a realistic scenario for the initial stages of deployment. Academic consideration has been given to scenarios where the maximum amount of energy is extracted from the Pentland Firth e.g. Ref. [22], in such cases turbines are arranged in lines which span the entire channel and sub-channels of the Pentland Firth. Clearly in this case, impacts on morphodynamics would be much greater given the greater levels of extraction and altered currents over a larger area. Engineering, geotechnical and marine spatial planning considerations mean that such proposals are unlikely to come to fruition at current level of technological development. If such plans become realistic then future work should investigate the impacts of these levels of extraction on sediment dynamics to facilitate consenting.

Areas suitable for tidal stream turbine deployment often have spatially varying sediment beds due to the varying current in the region: typically the main resource areas are swept rock with

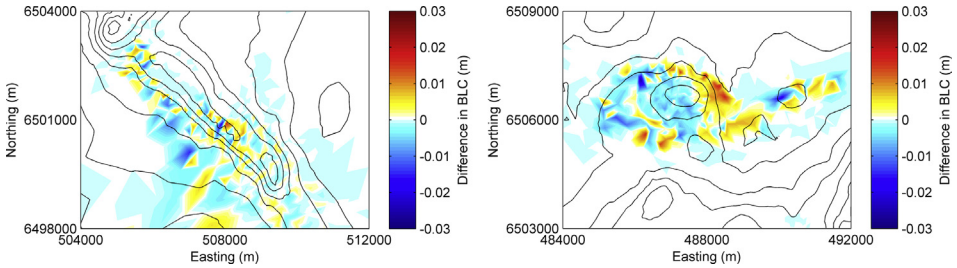

Fig. 18. A plot of the difference in impact on bed level for the case where all four farms are modelled at once and the case were the impacts of farms modelled individually are summed. The Sandy Riddle is shown on the left and the sand wave area on the right.

sediment deposits in the areas of lower flow. Not only will abundance vary, but sediment size is likely to vary too. In this study manual classification of the seabed type based on a textural surface was used. For clear cut areas of rippled sand or rock this method is effective but in less obvious locations it is likely that misclassification may have occurred. Where backscatter data is available as well as bathymetry, more sophisticated automated methods could be used [30]. It is suggested that data gathering in the Pentland Firth to enable a more rigorous seabed classification would be fruitful to aid future work. Another difficulty is that the depth of sediment deposit is largely unknown and can vary from several metres to a thin veneer. Sediment size data of varied quality was available to this study, while some relied on visual description it was believed that higher spatial resolution was more important than absolute accuracy.

Model results were analysed over one lunar month due in part to the availability in validation data and in part due to computational efficiency. This time period allows for the capture of the spring neap cycle and hence the hydrodynamic variation. However morphological changes can occur over much longer timescales of seasons to decades with responses being non-linear due to the influence of bed level on hydrodynamics. Given the minimal differences observed the monthly results are still believed to be of relevance, however it is possible that patterns of impact may change over longer time periods. A greater question is the impact of waves on sediment transport over these sandbanks, which were not included in these simulations. Studies conducted on offshore sandbanks on the south Wales coast [69] have suggested that sandbank volume changes are primarily related to storm conditions. Waves were not included in this contribution given the vast number of permutations of possible wave conditions that would need to be tested, however future work should consider this aspect. Not only would, under certain conditions, wave driven sediment transport alter or mask the tidally driven transport described here, but wave fields would potentially be modulated by changes to hydrodynamic conditions forced by renewable installations [70].

The results show that implementation of all four arrays have minimal impact on the morphology of the studied sub-tidal sandbanks in the Pentland Firth. While this finding must be qualified by the lack of accurate sediment data over the whole domain and the duration of the simulation, it is a positive result for the deployment of tidal stream turbines in the Pentland Firth. Other, smaller, sandbanks are present closer to the turbine deployment areas, and these are not studied in this contribution. It is likely that these will be affected by turbine implementation. For example [71], investigated a sandbank close to the Meygen array in the inner sound and found the sandbank was highly dynamic and maintained by residual currents and hence postulated that energy extraction would likely affect morphodynamics. The work presented here does not consider the very near field impact of tidal stream turbines on sediment dynamics. Depending on the seabed conditions at the turbine location, scour effects from the turbine foundations might be noted similar to that seen for offshore wind turbine foundations [72,73]. The presence of the rotor and its near field impact on flow will also cause local scouring of the seabed: both laboratory [74] and numerical studies [75,76] have demonstrated this. In Ref. [77] the authors showed that the extent of scour is limited to a narrow region extending a few rotor diameters downstream from the foundation. Very near field effects are less likely to be relevant in the Pentland Firth due to the fact that much of the footprint of the arrays is swept bedrock. Equally scour in reversing tidal currents is observed to be less significant than in mono-directional riverine flows due to partial infilling of scour holes with the reversing current [73].

The study suggests that cumulative impacts of multiple arrays are additive at the currently proposed levels of deployment. Should extraction levels increase such that blockage levels become larger this may well change. The results do show that the closest two farms do have some interaction in terms of hydrodynamic impact so if distance between farms were to be reduced; levels of non-linearity might increase.

7. Conclusions

The four currently proposed tidal stream turbine arrays in the Pentland Firth are modelled using a 3D numerical model and the impacts to morphodynamics compared to the modelled natural condition. Two primary areas of mobile sediment are considered: the Sandy Riddle and a sand wave field to the west of Stroma. Differences in bed level change between the turbine and natural case over the modelled lunar month are less than 0.2 m with all four farms activated. The root mean square difference between the natural and energy extraction case was 0.18 m over the sand wave area and 0.03 m over the Sandy Riddle. Compared to actual bed level changes of up to 5 m it is believed that this is insignificant. Consideration was given to the linearity of impact from multiple arrays: it was found that differences between the impacts of all four arrays modelled at once and the sum of impact of farms modelled individually was around 2 cm, root mean square differences were 0.03 m for the sand wave area and 0.02 m for the Sandy Riddle. This suggests that cumulative impacts of the four existing sites in the Pentland Firth will accumulate linearly for the currently proposed extraction levels. Both these results are very positive for the development of tidal stream energy extraction in the Pentland Firth. However it should be noted that if the scale of extraction was increased substantially from the currently proposed levels towards the upper limit of potential extraction, greater impacts would be observed and non-linearities in cumulative impact might be noted.

Acknowledgements

This work was supported by the EPSRC funded Terawatt project EP/J010170/1. The authors would like to thank BGS, the Crown Estate, UKHO and Marine Scotland for the data sharing with the Terawatt consortium. The two reviewers are thanked for their helpful suggestions.

References

[1] Ng K-W, Lam W-H, Ng K-C. 2002-2012: 10 Years of research progress in horizontal-axis Marine current turbines. Energies 2013;6:1497–526.
[2] Cummins PF. On the extractable power from a tidal channel. J Waterw Port Coast Ocean Eng Asce 2012;138:63–71.
[3] Defne Z, Haas KA, Fritz HM, Jiang L, French SP, Shi X, et al. National geodatabase of tidal stream power resource in USA. Renew Sustain Energy Rev 2012;16:3326–38.
[4] Fairley I, Evans P, Wooldridge C, Willis M, Masters I. Evaluation of tidal stream resource in a potential array area via direct measurements. Renew Energy 2013;57:70–8.
[5] Yates N, Walkington I, Burrows R, Wolf J. Appraising the extractable tidal energy resource of the UK's western coastal waters. Philos Trans R Soc A Math Phys Eng Sci 2013;371.
[6] Plew DR, Stevens CL. Numerical modelling of the effect of turbines on currents in a tidal channel – Tory Channel, New Zealand. Renew Energy 2013;57:269–82.
[7] Ramos V, Carballo R, Alvarez M, Sanchez M, Iglesias G. Assessment of the impacts of tidal stream energy through high-resolution numerical modeling. Energy 2013;61:541–54.
[8] Yang ZQ, Wang TP, Copping AE. Modeling tidal stream energy extraction and its effects on transport processes in a tidal channel and bay system using a three-dimensional coastal ocean model. Renew Energy 2013;50:605–13.
[9] Masters I, Malki R, Williams AJ, Croft TN. The influence of flow acceleration on tidal stream turbine wake dynamics: a numerical study using a coupled BEM-CFD model. Appl Math Model 2013;37:7905–18.

[10] Schlezinger DR, Taylor CD, Howes BL. Assessment of zooplankton injury and mortality associated with underwater turbines for tidal energy production. Mar Technol Soc J 2013;47:142–50.
[11] Waggitt JJ, Scott BE. Using a spatial overlap approach to estimate the risk of collisions between deep diving seabirds and tidal stream turbines: a review of potential methods and approaches. Mar Policy 2014;44:90–7.
[12] Martin-Short R, Hill J, Kramer SC, Avdis A, Allison PA, Piggott MD. Tidal resource extraction in the Pentland Firth, UK: potential impacts on flow regime and sediment transport in the inner sound of Stroma. Renew Energy 2015;76:596–607.
[13] Neill SP, Litt EJ, Couch SJ, Davies AG. The impact of tidal stream turbines on large-scale sediment dynamics. Renew Energy 2009;34:2803–12.
[14] Neill SP, Jordan JR, Couch SJ. Impact of tidal energy converter (TEC) arrays on the dynamics of headland sand banks. Renew Energy 2012;37:387–97.
[15] Robins PE, Lewis MJ, Neill SP. Impact of tidal-stream arrays in relation to the natural variability of sedimentary processes. Renew Energy. Accepted to (2014).
[16] MeyGen. MeyGen tidal energy project – phase 1: environmental statement. 2012.
[17] Easton MC, Woolf DK, Bowyer PA. The dynamics of an energetic tidal channel, the Pentland Firth, Scotland. Cont Shelf Res 2012;48:50–60.
[18] Osborn GR, Hinton CL, Cooper WS. Pentland Firth and Orkney Waters strategic area: marine energy resources. In: ABPmer/the Crown estate; 2012.
[19] Saruwatari A, Ingram DM, Cradden L. Wave-current interaction effects on marine energy converters. Ocean Eng 2013;73:106–18.
[20] Draper S, Adcock TAA, Borthwick AGL, Houlsby GT. Estimate of the tidal stream power resource of the Pentland Firth. Renew Energy 2014;63:650–7.
[21] Garrett C, Cummins P. The power potential of tidal currents in channels. Proc R Soc A Math Phys Eng Sci 2005;461:2563–72.
[22] Adcock TAA, Draper S, Houlsby GT, Borthwick AGL, Serhadlioglu S. The available power from tidal stream turbines in the Pentland Firth. Proc R Soc A Mathe Phys Eng Sci 2013;469.
[23] Johnson MA, Kenyon N, Belderson RH, Stride AH. Sand transport. In: Stride AH, editor. Offshore tidal sands. Processes and deposits. Chapman and Hall; 1982. p. 58–94.
[24] Farrow GE, Allen NH, Akpan EB. Bioclastic carbonate sedimentation on a high latitude, tide-dominated shelf: northeast Orkney Islands, Scotland. J Sediment Petrol 1984;54:373–93.
[25] Light JM, Wilson JB. Cool-water carbonate deposition on the West Shetland Shelf: a modern distally steepened ramp. Special Publication Geol Soc 1998;149:73–105.
[26] Flather RA. Estimates of extreme conditions of tide and surge using a numerical model o the north-west European continental shelf, Estuarine. Coast Shelf Sci 1987;24:69–93.
[27] Kenyon NH, Cooper B. Sand banks, sand transport and offshore windfarms. 2005.
[28] ABPmer. Pentland Firth and Orkney Waters strategic area: preparation of bathymetry to support modelling studies. In: The Crown Estate; 2012.
[29] Ahmed KI, Demsar U. Improving seabed classification from multi-beam echo sounder (MBES) backscatter data with visual data mining. J Coast Conserv 2013;17:559–77.
[30] Micallef A, Le Bas TP, Huvenne VAI, Blondel P, Huehnerbach V, Deidun A. A multi-method approach for benthic habitat mapping of shallow coastal areas with high-resolution multibeam data. Cont Shelf Res 2012;39–40:14–26.
[31] Folk RL, Andrews PB, Lewis DW. Detrital sedimentary rock classification and nomenclature for use in New Zealand. N Z J Geol Geophys 1970;13:937–68.
[32] DHI, in, 2014.
[33] Abbaspour M, Rahimi R. Iran atlas of offshore renewable energies. Renew Energy 2011;36:388–98.
[34] Lalander E, Leijon M. In-stream energy converters in a river – effects on upstream hydropower station. Renew Energy 2011;36:399–404.
[35] Venugopal V, Bryden IG, Wallace AR. Asme, on the interaction of waves with an array of open chambered structures: application to wave energy converters. 2010.
[36] Osborn GR, Hinton CL, Cooper WS. Pentland Firth and Orkney Waters hydrodynamic modelling: model calibration. In: ABPmer/the Crown estate; 2012.
[37] Fairley I, Davidson M, Kingston K. The morpho-dynamics of a beach protected by detached breakwaters in a high energy tidal environment. J Coast Res 2009:607–11.
[38] Martinelli L, Zanuttigh B, Lamberti A. Analysis of coastal flooding hazard in a low-lying area of the Northern Adriatic Sea, Italy. 2009.
[39] Siegle E, Huntley DA, Davidson MA. Coupling video imaging and numerical modelling for the study of inlet morphodynamics. Mar Geol 2007;236:143–63.
[40] DHI, MIKE 21 and MIKE 3 flow model FM – hydrodynamic and transport module – scientific documentation. 2012.
[41] DHI, MIKE 3 flow model FM – hydrodynamic module – user guide. In: DHI; 2012. p. 130.
[42] Smagorisky J. General circulation experiment wit the primitive equations. Mon Weather Rev 1963;91:99–164.
[43] DHI, MIKE3 flow model FM – sand transport module – user guide. In: DHI; 2012.
[44] van Rijn LC. Sediment transport, part 1: bed load transport. J Hydraulic Eng 1984;110:1431–56.
[45] van Rijn LC. Sediment transport, Part II: suspended load transport. J Hydraulic Eng 1984;110:1613–41.
[46] Adcock TAA, Borthwick AGL, Houlsby GT. The open boundary problem in tidal basin modelling with energy extraction. In: EWTEC, Southampton; 2011.
[47] Baston S, Harris RE. Modelling the hydrodynamic characteristics of tidal flow in the Pentland Firth. In: EWTEC 2011, Southampton; 2011.
[48] DHI, email communication regarding turbine implementation, in: I. Fairley (Ed.), 2015.
[49] Zori LAJ, Rajagopalan RG. Navier-Stokes calculations of rotor-airframe interaction in forward flight. J Am Helicopter Soc 1995;40:57–67.
[50] Molland AF, Turnock SR, Wilson PA. Performance of an enhanced rudder force prediction model in a ship manoeuvring simulator. 1996.
[51] Newman BG. Multiple actuator-disk theory for wind turbines. J Wind Eng Ind Aerodyn 1986;24:215–25.
[52] Hansen MOL, Sorensen JN, Voutsinas S, Sorensen N, Madsen HA. State of the art in wind turbine aerodynamics and aeroelasticity. Prog Aerosp Sci 2006;42:285–330.
[53] Batten WMJ, Harrison ME, Bahaj AS. Accuracy of the actuator disc-RANS approach for predicting the performance and wake of tidal turbines. Philos Trans Royal Soc London A: Math Phys Eng Sci 2013;371.
[54] Baston S, Waldman S, Side J. Modelling energy extraction in tidal flows. 2014.
[55] Myers LE, Bahaj AS. Experimental analysis of the flow field around horizontal axis tidal turbines by use of scale mesh disk rotor simulators. Ocean Eng 2010;37:218–27.
[56] Myers LE, Bahaj AS. An experimental investigation simulating flow effects in first generation marine current energy converter arrays. Renew Energy 2012;37:28–36.
[57] Nishino T, Willden RHJ. Two-scale dynamics of flow past a partial cross-stream array of tidal turbines. J Fluid Mech 2013;730:220–44.
[58] Nishino T, Willden RHJ. Low-order modelling of blade-induced turbulence for RANS actuator disk computations of wind and tidal turbines. In: Holling M, Peinke J, Ivanell S, editors. Wind energy – impact of turbulence. Springer; 2014.
[59] Garrett C, Cummins P. Generating power from tidal currents. J Waterw Port Coast Ocean Eng Asce 2004;130:114–8.
[60] Houlsby GT, Draper S, Oldfield MGL. Application of linear momentum actuator disc theory to open channel flow. Oxford: Univeristy of Oxford, Department of Engineering Science; 2008. p. 25.
[61] Whelan JI, Graham JMR, Peiro J. A free-surface and blockage correction for tidal turbines. J Fluid Mech 2009;624:281–91.
[62] ScottishPowerRenewables. Proposed Ness of Duncansby tidal array request for a scoping opinion. 2012.
[63] Easton MC, Woolf DK. The influence of non-linear turbine dynamics on the environmental stress of tidal stream arrays. In: EWTEC 2013, Aalborg; 2013.
[64] Ahmadian R, Falconer RA. Assessment of array shape of tidal stream turbines on hydro-environmental impacts and power output. Renew Energy 2012;44:318–27.
[65] Malki R, Masters I, Williams AJ, Nick Croft T. Planning tidal stream turbine array layouts using a coupled blade element momentum – computational fluid dynamics model. Renew Energy 2014;63:46–54.
[66] Stallard T, Collings R, Feng T, Whelan J. Interactions between tidal turbine wakes: experimental study of a group of three-bladed rotors. Philos Trans R Soc A Math Phys Eng Sci 2013;371.
[67] Edmunds M, Malki R, Williams AJ, Masters I, Croft TN. Aspects of tidal stream turbine modelling in the natural environment using a coupled BEM–CFD model. Int J Mar Energy 2014;7:20–42.
[68] Funke SW, Farrell PE, Piggott MD. Tidal turbine array optimisation using the adjoint approach. Renew Energy 2014;63:658–73.
[69] Lewis MJ, Neill SP, Elliott AJ. Interannual variability of two ofshore sand banks in a region of extreme tidal range. J Coast Res 2015;31(2):265–75.
[70] Fairley I, Ahmadian R, Falconer RA, Willis MR, Masters I. The effects of a Severn Barrage on wave conditions in the Bristol Channel. Renew Energy 2014;68:428–42.
[71] Chatzirodou AC, Karunarathna H. Impacts of tidal energy extraction on sea bed morphology. In: ICCE 2014, Seoul, Korea; 2014.
[72] Harris JM, Whitehouse RJS, Benson T. The time evolution of scour around offshore structures. Proc Inst Civ Engineers-Maritime Eng 2010;163:3–17.
[73] McGovern DJ, Ilic S, Folkard AM, McLelland SJ, Murphy BJ. Time development of scour around a cylinder in simulated tidal currents. J Hydraulic Eng 2014;140.
[74] Hill C, Musa M, Chamorro LP, Ellis C, Guala M. Local scour around a model hydrokinetic turbine in an erodible channel. J Hydraulic Eng 2014;140.
[75] Chen L, Lam WH. Slipstream between marine current turbine and seabed. Energy 2014;68:801–10.
[76] Vybulkova L. A study of the wake of an isolated tidal turbine with application to its effects on local sediment transport. Glasgow: School of Engineering, University of Glasgow; 2013.
[77] Williams AJ, Croft TN, Masters I, Willis MR. Investigating environmental issues related to operation of tidal stream turbines using a BEM-CFD model. In: Sayigh AAM, editor. World renewable energy Congress XI Abu Dhabi, UAE; 2010.